

Molecular Origin of Hydration Heat Capacity Changes of Hydrophobic Solutes: Perturbation of Water Structure around Alkanes

Bhupinder Madan and Kim Sharp*

The Johnson Research Foundation, Department of Biochemistry and Biophysics, University of Pennsylvania, Philadelphia, Pennsylvania 19104-6059

Received: July 28, 1997; In Final Form: October 8, 1997[®]

The heat capacities of hydration (ΔC_p) of the first four of the linear alkane series, methane, ethane, propane, and butane, were calculated by a combination of Monte Carlo simulations and the random network model (RNM) of water. The contribution from the water–water interaction and the solute–water interaction accounted for about 45% and 20%, respectively, of the experimental values. The water–water contribution to ΔC_p arises from distortions in the water structure in the hydration shell. The hydrogen bonds between the water molecules in the first hydration shell were shorter and less bent (had a smaller root-mean-square angle, θ) compared to those in pure water. In the case of propane and butane, the greatest decrease in θ was for waters hydrating the methyl groups, with a somewhat smaller decrease for waters hydrating the methylene groups. Thus the contribution to ΔC_p per hydrogen bond from water around the methyl groups is a little larger than from water around the methylene groups. This also implies that the hydrogen bonds around the former are slightly stronger than those around the latter. The calculated ΔC_p for the four hydrocarbons depends nearly linearly on the number of hydrogen bonds participating in the first hydration shell of each solute, which in turn depends linearly on the total accessible surface area of the molecule or the number of carbon atoms in the hydrocarbon. It is evident, however, that the number of hydrogen bonds in the first shell characterizes the hydration heat capacity better than the total accessible surface area of the solute does. This is so because the number of hydrogen bonds with their RNM parameters not only gives a good estimate for the hydration heat capacities but also provides an insight to the mechanism for such an effect.

1. Introduction

Heat capacities of hydration (ΔC_p) have become an important area of study because they are a major, if not the major, contributor to heat capacity changes in a variety of important phenomena, including small solute solvation, the hydrophobic effect—one of the main stabilizing interactions in proteins, in the determination of protein stability as a function of temperature and amino acid composition, and in the dissection of the energetics of protein folding and protein–ligand binding.^{1,2} Until recently, it was extremely difficult to study hydration heat capacity changes from a theoretical point of view because of the difficulty in obtaining reliable heat capacity estimates from simulations. In a recent pair of papers (I, II),^{3,4} we have successfully introduced a methodology to compute the water–water interaction contribution to heat capacity changes for the hydration of hydrophobic, polar, and mixed group molecules and single atom and multiatom ions. In paper I, we also obtained a very good estimate for the total heat capacity change of hydration for a simple hydrophobic solute, Ar, including the contribution due to the solute–solvent interaction. We have shown that the experimentally observable effect, namely that the heat capacity changes for the hydration of hydrophobic groups and polar groups or ions are in the opposite directions, can be reproduced quite satisfactorily by using a combination of the random network model (RNM) of water and Monte Carlo simulations of dilute aqueous solutions of these solutes.

The opposite signs of changes in the heat capacity of hydration are explicable in terms of the effect of polar and nonpolar solute groups on the length and angle of hydrogen bonds between water molecules in the first hydration shell. We

previously observed that, around nonpolar groups, the water–water hydrogen bond length and root-mean-square of hydrogen bond angles decrease relative to pure water, while the opposite effect occurs around polar and ionic groups. These changes result from changes in the relative amounts of two populations of hydrogen bonds, one with shorter, more linear bonds, the other with longer, less linear bonds. Changes in bond length and angle induced by polar and nonpolar solutes are highly concerted. Overall, this provides a unified picture of polar and nonpolar hydration heat capacity changes. From these studies, we have suggested that the opposite sign in the changes in the heat capacity of hydration for apolar and polar groups is the most useful distinction between hydrophobic and polar solvation, and that study of heat capacity changes provides a better insight into the role of changes in water structure upon hydration than analysis of entropy or enthalpy changes alone.

A common procedure for estimating the heat capacity and other thermodynamic quantities of hydration of various molecules, including amino acids, is to parametrize these properties against the water accessible surface area of these molecules. This is often a successful method because it takes into account the predominant interaction of the solute with the water molecules in the nearest hydration shell, which scales well with the solvent accessible area. But this is a highly phenomenological method which does not shed light on the reason of its success, other than the fact that the water in the hydration shell is responsible for the various thermodynamic properties of hydration. The success of the random network model and Monte Carlo simulations in predicting the heat capacity of hydration for various molecules now allows us to investigate in more detail the correlation between the water accessible surface area of hydrophobic solutes, the number of water–water hydrogen bonds, in the first hydration shell, which are perturbed,

* To whom correspondence should be addressed.

[®] Abstract published in *Advance ACS Abstracts*, December 1, 1997.

and the magnitude of the resulting heat capacity changes. For this purpose, the linear alkane series, being a homologous, entirely nonpolar and well-studied solute series, provides an ideal choice.

In this work, we have set out to accomplish two goals: first, to determine the magnitude of the heat capacity changes for the hydration of a series of alkane molecules and, second, to offer a more structural interpretation of the dependence of the heat capacity changes on the accessible surface area. In the next section, we briefly describe the theory and the methodology already explained in detail in our previous work. The extension of the RN model to study heat capacity changes developed in the previous two papers is described briefly. In the Methods section, we describe the simulation procedures and the methods employed to compute the RN model parameters in the bulk water and in the hydration shells of solutes. In the following section, we give the heat capacity results from the combined RN model and the Monte Carlo simulations. We also give results on the reorganization of water around the various methyl and methylene groups in the four alkane molecules in terms of the RN model parameters. The discussion of the results follows in the same section. Since RN model parameters for the hydrogen bonds in the first shell of each of these hydrocarbons is more or less same; we emphasize that the number of hydrogen bonds in the first shells of each of these hydrocarbons is representative of the magnitude of the heat capacity changes occurring in these systems. We further show that this number is proportional to the accessible surface area. Therefore, the number of hydrogen bonds in the first hydration shell of hydrocarbons gives a clearer picture compared to the various methods based on parametrizing the heat capacity changes as a function of the accessible surface area.

2. Theory

The heat capacity, C_p , relates the other three major thermodynamic quantities, enthalpy (H), entropy (S), and free energy (G), to each other

$$C_p = \frac{\partial H}{\partial T} = T \frac{\partial S}{\partial T} = -T^2 \frac{\partial^2 G}{\partial T^2} = \frac{\langle \Delta H^2 \rangle}{kT^2} \quad (1)$$

(i) (ii) (iii) (iv)

where T is the temperature, k is Boltzmann's constant, and $\langle \Delta H^2 \rangle$ is the mean squared fluctuation in enthalpy. The heat capacity of hydration is a complex quantity to determine directly from computer simulations for two reasons. First, as is evident from eq 1, the heat capacity of even a simple system is time consuming to determine from the simulations because it requires determination of the second derivative of the free energy, the first derivative of the enthalpy, or the fluctuations in the enthalpy of the system. Using the latter approach, for example, the relatively small systems required for practical computer simulation lengths are not suitable for computation of heat capacity because it takes a long time for fluctuational quantities to converge in these type of simulations. Second, the process of hydration adds an additional difficulty: one has to take a difference in heat capacity between pure water, and water plus a solute. If the simulated system is made larger in order to reproduce fluctuational quantities better, one is trying to evaluate a small difference between two increasingly large heat capacity values. To avoid the difficulties associated with this type of brute force approach we have adopted an alternative strategy.

The heat capacity changes for hydration can be divided into three components arising from three contributions to the mean energy: the intramolecular solute interaction (E^{ss}), the direct

solute–solvent contribution (E^{sv}), and an indirect contribution arising from changes in water–water interaction induced by the solute (ΔE^{vv}). The intramolecular solute interaction refers to the interaction between atoms or groups within the same solute molecule. For an infinitely dilute solution, which is what we are interested in, there is no intermolecular solute–solute interaction. Thus, from eq 1, i, the three corresponding contributions to the heat capacity change can be expressed in the following equation:

$$\Delta C_p = \left(\frac{\partial E^{\text{ss}}}{\partial T} \right)_p + \left(\frac{\partial \Delta E^{\text{sv}}}{\partial T} \right)_p + \left(\frac{\partial \Delta E^{\text{vv}}}{\partial T} \right)_p = C_p^{\text{ss}} + \Delta C_p^{\text{sv}} + \Delta C_p^{\text{vv}} \quad (2)$$

The contribution from the $P\Delta V$ term has not been included because at 1 atm, $P = 4.46 \times 10^{-5}$ kJ/mL/mol, so for the hydration of most solutes, where the molar volumes are 10s to 100s of mL/mol, this term is negligible. For small solutes and even for proteins it has been argued,^{5,6} $C_p^{\text{ss}} \approx 0$. The second term can be obtained from a straightforward computation of the difference in solute–water interaction energy (E^{sv}) at various temperatures. The third term, ΔC_p^{vv} , is due to the changes in the water–water interaction energy (ΔE^{vv}); this arises from the changes in the hydrogen bond network of the water shell around polar and nonpolar solutes as compared to the H-bond network of bulk water. This last term is the most interesting and elusive and it has been computed in our previous work^{3,4} by a combination of Monte Carlo and random network model of water for various polar and nonpolar solutes.

The random network (RN) model of water has successfully reproduced various physical properties of water, including thermodynamic properties such as entropy and the heat capacity, the radial distribution function, the temperature dependence of the dielectric constant, and the isothermal compressibility of water.^{7,8} In this model, equations of state for various thermodynamic properties of water are derived from various ice data, using the observation that even liquid water has much of the tetrahedral H-bonding network of ice I. The model further assumes that the essential features of this network in water can be described in terms of just three structural parameters, the mean and the standard deviation in H-bond length, d , and s , respectively, and the root-mean-square (rms) H-bond angle, θ .^{7,8} The H-bond length is the distance between oxygen atoms of the two water molecules which are hydrogen bonded. The H-bond angle is the angle between the inter oxygen atom axis and that oxygen–hydrogen axis which forms the smallest angle. The accurate equations of state for the free energy, enthalpy, and entropy of pure liquid water have been obtained from the RN model^{9–11} and these relations have then been used to obtain an equation of state for the heat capacity in terms of the RN model structural parameters³

$$C_p^{\text{rn}}(d, s, \theta) = C_p^{\text{bend}}(d, s, \theta) + C_p^{\text{stretch}}(d, s, \theta) + C_p^{\text{vib}}(d, s, \theta) \quad (3)$$

with contributions from H-bond bending, stretching, and vibrations, C_p^{bend} , C_p^{stretch} , and C_p^{vib} , respectively. This equation of state for the heat capacity has been applied to compute the water–water interaction contribution to the heat capacity of hydration of various nonpolar, polar, and single atom as well as multiatom ionic solutes in our previous work. Each of these solute molecule perturbs the H-bonding structure of the surrounding water, mostly of water molecules in the first hydration shell of the solute molecules. The total heat capacity change produced due to changes in the surrounding H-bond network by a solute is computed, using eq 3, by summing the contribu-

tions from all of the perturbed hydrogen bonds in the following manner:

$$\Delta C_p^{\text{hyd}} = \sum_i N_i [C_p^{\text{m}}(d_i, s_i, \theta_i) - C_p^{\text{m}}(d_0, s_0, \theta_0)] = \sum_i N_i \Delta C_p^{\text{m}}(d, s, \theta) \quad (4)$$

where C_p^{m} is the contribution to heat capacity arising from a group of N_i perturbed H bonds with average parameters d_i , s_i , and θ_i , where d_0 , s_0 , and θ_0 are the corresponding values for the bulk water in the absence of solute. An increase in H-bond length and angle has been found to decrease the water heat capacity contribution, while decreases in length and angle have been found to cause the opposite effect.

3. Methods

Dilute aqueous solutions of four alkanes, methane, ethane, propane, and butane, were studied. Each of the four systems had 750 water molecules. In addition, the solutions contained one molecule of solute. The water model used was TIP4P and the parameters for the solute molecules were OPLS parameters.^{12,13} The systems were equilibrated at 1 atm pressure and 25 °C for 5×10^7 Monte Carlo steps. The equilibrated configurations were then run over 10 consecutive runs of 1×10^7 MC steps to compute averages and standard deviations of the random network model parameters and solute–solvent interaction energies. The computer program used to generate the configurations for the solution systems was the Monte Carlo program BOSS version 3.3.¹⁴ Snapshots were chosen every 1000 steps to compute the RN model parameters and the solute–solvent interaction energy.

The RN model parameters (d , s , and θ) were obtained for all H bonds within the first hydration shell as follows. The first hydration shell is defined as all the water molecules within the first minimum of the solute–water radial distribution functions. The length and angle of H bonds were computed for each pair of waters in this shell that were H bonded. Two water molecules are deemed to be H bonded if they lie within a distance of 3.4 Å, the first minimum in the O–O radial distribution function of pure water. The above definition of a hydrogen bond permits the inclusion of distortions in the H-bonding network, particularly angular distortions, that in the RN model are responsible for the heat capacity changes. The distances and angles were binned and accumulated over the course of the simulation to produce their probability distribution functions which were then used to compute the mean and the standard deviation in H-bond length, d and s , respectively, and the root-mean-square (rms) H-bond angle, θ . The number of hydrogen bonds between the water molecules in the first hydration shell (N_{11}) was counted and averaged over the individual runs. The RN model parameters for pure water (d_0 , s_0 , and θ_0) used here were obtained from the previous work.³ The contribution due to water–water interaction toward the total heat capacity change for hydration was computed in the following manner. The RN model parameters (d , s , and θ), for the pure water and water surrounding solutes in their solutions, obtained from the simulations are uniformly scaled so that the values for pure water obtained from the simulations match those obtained self-consistently from the RN model applied to pure water.⁸ This enables us to obtain *changes* in heat capacity while ensuring consistency between our simulations and the RN model for pure water. The scaled values were used in the eqs 2 and 3 to obtain the contribution due to the water–water interactions toward the change in the heat capacity of hydration.

TABLE 1: Averaged Random Network Model (RNM) Parameters for H Bonds among Water Molecules in the First Hydration Shell of Alkanes

solute	mean H-bond length (d), Å	std dev in H-bond length (s), Å	rms H-bond angle (θ), deg	ΔC_p^{vv} per H bond, cal/(mol K)
bulk water	2.94 ± 0.001	0.22 ± 0.0003	29.4 ± 0.1	
methane	2.91 ± 0.005	0.21 ± 0.001	24.4 ± 0.4	0.84
ethane	2.91 ± 0.007	0.21 ± 0.002	24.6 ± 0.9	0.78
propane	2.91 ± 0.01	0.21 ± 0.004	24.5 ± 1.2	0.79
butane	2.91 ± 0.01	0.21 ± 0.004	24.7 ± 1.1	0.78

The solute–solvent interactions were calculated in three parts: solute–first shell water energy, E^{s1} , solute–second shell water energy, E^{s2} , and solute–third shell (bulk) water energy, E^{s3} . These contributions too were averaged over the 10 runs, each run of 1×10^7 MC steps. Temperature derivatives were obtained numerically by evaluating E^{s} from simulations run at 278, 298, and 318 K and taking the difference. Only solute–first shell and solute–second shell values were used in the final computation of heat capacities. The solute–third shell (bulk water) interaction energies were rejected for reasons of statistical precision, due to the high standard deviations and small absolute values of E^{s3} .

4. Results and Discussion

The effect of the alkanes on the water structure is shown in Table 1. All the solutes decreased the mean hydrogen bond length and rms angle compared to bulk water. The decrease is indistinguishable between the different hydrocarbons, indicating little effect of solute size on the water structure. The constant pressure heat capacities, C_p , of hydration of four hydrocarbons are found to be in reasonably good agreement with the experimental values as shown in Table 2. The contributions toward the heat capacity of hydration due to the water–water interactions are about 45% of the experimental values. The contributions due to the solute–water interactions are about 20% of the experimental values. Overall, our simulations reproduce the observed trend in heat capacity but underestimate the experimental values by about 35% (Figure 1). A possible cause for the smaller computed values compared to the experimental values has been investigated in the earlier studies.^{3,4} It was observed that the random network model (RNM) parameters for (i) the hydrogen bonds formed between one water molecule belonging to the first hydration shell and another water molecule in the second hydration shell (1–2 H bonds) and for (ii) the hydrogen bonds formed between both water molecules belonging to the second hydration shell (2–2 H bonds) were almost equal to the RNM parameters of bulk water. This gave a zero contribution from the water–water interaction to the heat capacity of hydration from such hydrogen bonds i.e., 1–2 H bonds and 2–2 H bonds. Hydrogen bonds belonging to these two classes would make a significant contribution to the heat capacity even if they were perturbed slightly, compared to bulk water, because there are a larger number of these hydrogen bonds than between water molecules in the first hydration shell. Much longer simulations are required to obtain statistically reliable estimates of these small changes in the RNM parameters for 1–2 H bonds and 2–2 H bonds as compared to the RNM parameters of H bonds in bulk water. This is consistent with the underestimates of the heat capacity values from the experiments. Another plausible cause for the discrepancy between the computed values and the experimental values could be the fact that two different models for water have been combined in our studies. In the random network model of water,

TABLE 2: Heat Capacity of Hydration for Alkanes from RNM Model and Experiments^a

solute	no. of hydrogen bonds in first shell	solvent-accessible surface area (Å ²)	water–water heat capacity change	solute–water heat capacity change	total heat capacity change	
					calcd	measd
methane	25.54 ± 0.7	120.8	21.6 ± 1.9	8.1 ± 2.1	29.7 ± 4.0	49.6
ethane	34.78 ± 1.8	150.3 ± 0.4	27.0 ± 2.9	11.7 ± 2.2	38.7 ± 5.1	60.0
propane	39.83 ± 1.7	178.0 ± 1.3	31.3 ± 5.3	12.1 ± 3.4	43.4 ± 8.7	70.5
butane	49.65 ± 1.6	201.9 ± 2.6	38.6 ± 6.6	12.6 ± 0.3	51.2 ± 6.9	89.2

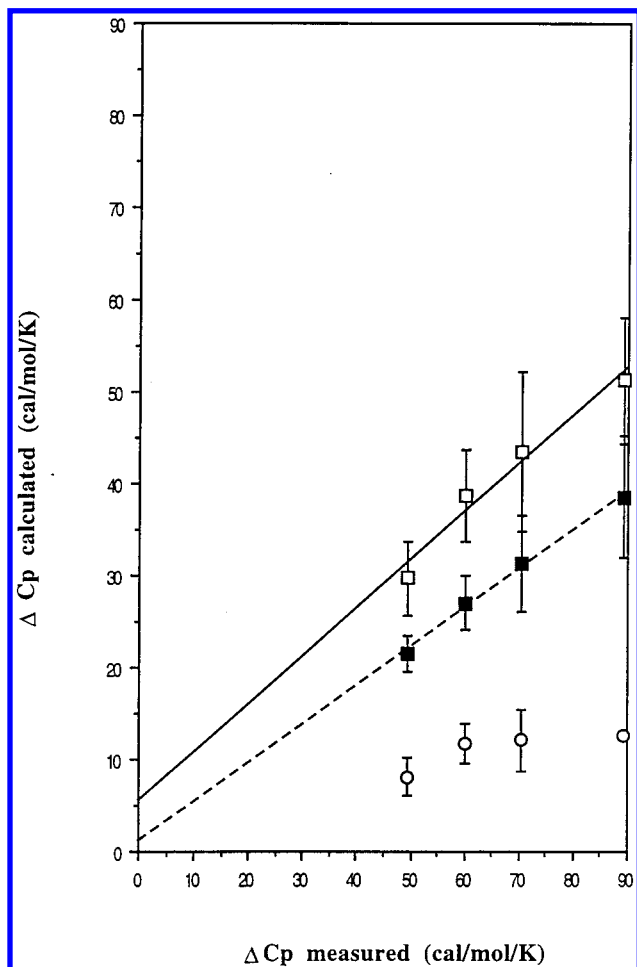
^a Heat capacities in cal/(mol K).

Figure 1. Comparison of experimental and calculated heat capacities of hydration for linear alkanes. Closed squares denote the contribution due to the water–water interactions, open circles denote the contribution due to the solute–water interaction, and open squares denote the total heat capacity of hydration of alkanes. Values for hydration of methane, ethane, propane, and butane are plotted left to right in each category. The fit for the contribution due to the water–water interactions is $y = 1.109 + 0.423x$, $R^2 = 0.95$. The fit for the total heat capacity of hydration is $y = 5.541 + 0.523x$, $R^2 = 0.966$.

the expression for the heat capacity of water in terms of the random network parameters is obtained by parametrizing the energy function of ice and water from their physical properties. While in our study the random network parameters of water were obtained by simulations of TIP4P water. Obviously, the average values of the random network parameters for the two models are not exactly equal to each other. However, consistency was reached by uniformly scaling the random network parameters of TIP4P water in bulk and around solutes such that the values for bulk water obtained from the simulations match those obtained self-consistently from the RNM applied to pure water. We believe that still better results may be achieved if a RN model like expression for the energy of TIP4P water as a function of its random network model parameters was derived.

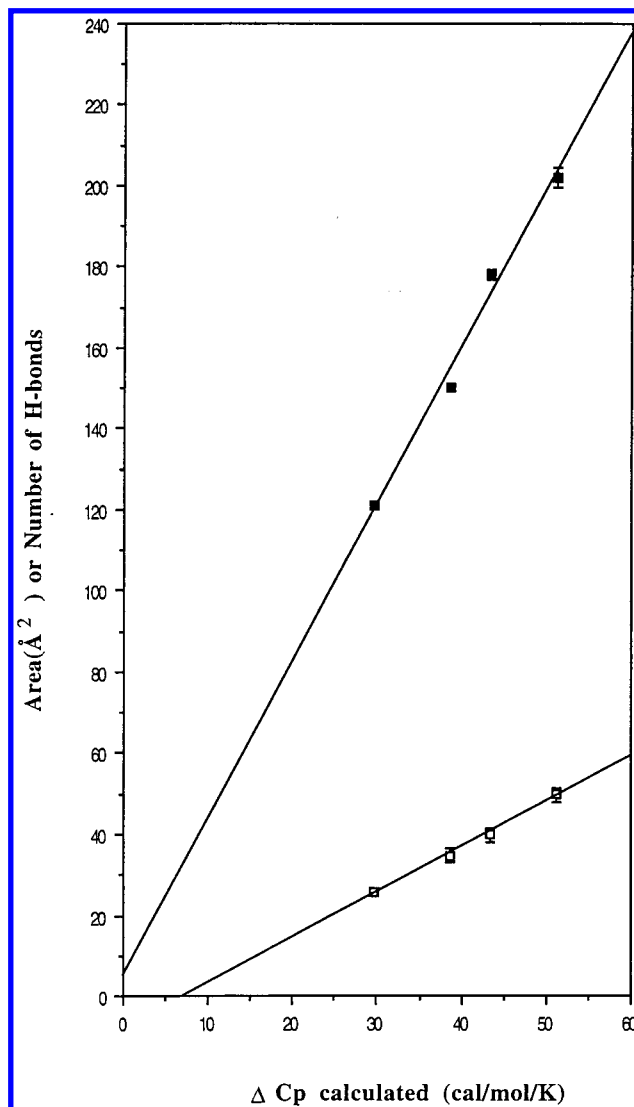


Figure 2. Relationship between number of first shell water–water hydrogen bonds, solvent-accessible surface area, and the calculated hydration heat capacity of four alkanes. Closed squares denote the average solvent accessible surface area and the open squares denote the number of hydrogen bonds in the first hydration shell. Values for hydration of methane, ethane, propane, and butane are plotted left to right in both cases. The fit for the solvent accessible surface area is $y = 5.012 + 3.871x$, $R^2 = 0.987$. The fit for the number of hydrogen bonds in the first hydration shell is $y = -8.06 + 1.117x$, $R^2 = 0.997$.

Such a study is in progress. In spite of the fact that the computed values reported here are underestimates of the experimental values, this study represents, to our knowledge, only direct and statistically reliable simulation of hydration heat capacities of a linear alkane series.

The water–water contributions to the hydration heat capacity are linear functions of the number of hydrogen bonds participating in the first shells of each of the hydrocarbon, of the SAS of the solutes (Figure 2). The linear dependence of the heat

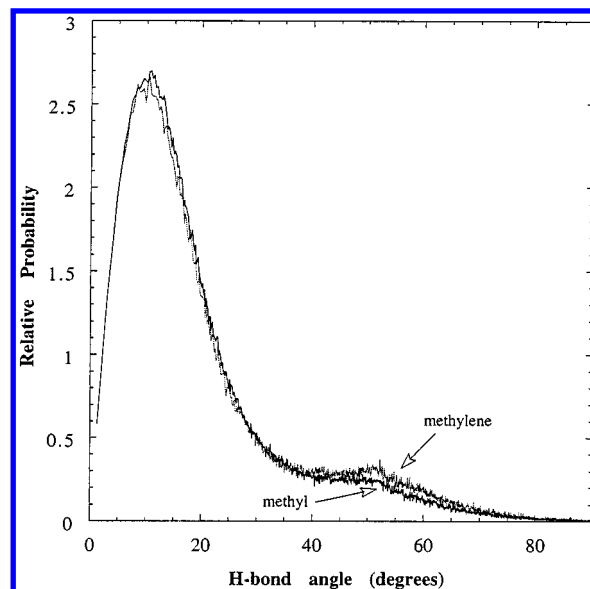
TABLE 3: Comparison of Random Network Parameters and Heat Capacity Contribution for Methyl and Methylene Groups in Propane and Butane^a

solute	group being hydrated	mean H-bond length (d)	std dev in H-bond length (s)	rms H-bond angle (θ)	ΔC_p^{vv} per H-bond (cal/mol/K)
propane	methyl	2.90	0.21	23.57	0.99
	methylene	2.91	0.21	25.12	0.74
butane	methyl	2.90	0.21	23.79	0.98
	methylene	2.90	0.21	24.85	0.82

^a Lengths in Å, angle in deg.

capacity on the number of hydrogen bonds among the water molecules in the first hydration shell is a result of the fact that the random network model parameters for the hydrogen bonds among water molecules of the first hydration shell of each of the solutes have almost identical values while the number of water molecules in the hydration shell increases with the hydrocarbon size. Our analysis also shows that the temperature variation of the mean energy of solute–water interaction contributes about 20% of the heat capacity change. Interestingly, this contribution also scales approximately linearly with SAS probably because the solute–solvent interaction is primarily a short-ranged van der Waals interaction, which will scale approximately with the number of waters in the first shell, and hence with SAS.

In computing the total heat capacity change, the random network model parameters for H bonds for the water molecules around these solutes are averaged over all the hydrogen bonds among all the water molecules in the first hydration shell regardless of the fact which group, methyl or methylene, they belong to. A closer analysis shows small but significant differences in random network model parameters for the methyl groups at the end of the chain as opposed to that for the methylene groups in the middle of the chain (Table 3). The rms hydrogen bond angle (θ) has a smaller value for water molecules around the methyl groups at the end of the chain than around the methylene groups in the middle of the chain. This effect is explainable in purely geometrical terms. There are a larger number of water molecules and hence a larger number of hydrogen bonds in the first shell around methyl groups than that around the methylene groups. The more exposed position of waters around the terminal groups provides more freedom for these waters to adopt optimal positions, resulting in a kind of cooperative straightening of hydrogen bonds. In contrast, the water molecules around the methylene groups in the middle of the chain have to form the best possible hydrogen bonds among themselves and with the water molecules at the nearby edge of the first hydration shell of the methyl groups, resulting in less optimal, and perhaps weaker, hydrogen bonding. Thus the contributions per hydrogen bond toward the hydration heat capacity are slightly different from these two groups. The conjecture that the hydrogen bonds among water molecules around the methyl groups are stronger than the hydrogen bonds among water molecules around methylene groups is also supported by the probability distribution plots of hydrogen bond angles for different sets of hydrogen bonds (Figure 3). There are two peaks. The major one centered around 12° arises from the waters coordinated in a roughly tetrahedral fashion around a central water molecule. The smaller peak at 52° arises from the occasional fifth water that forms part of the coordination shell of the central water. The probability distribution of hydrogen bond angles for hydrogen bonds around methyl groups shows a significantly smaller peak around 52° compared to the methylene group probability distribution.

**Figure 3.** Hydrogen bond angle probability distributions for first hydration shell of water around methyl and methylene groups of propane.

The concept of solvent-accessible surface area (SAS) introduced by Lee and Richards¹⁵ has stimulated a number of studies that relate various measures of hydrophobicity to the solvent accessible surface area in hydrocarbons, amino acids and proteins. Earlier quantitative studies of hydrophobicity focused on the correlation of solvent accessible surface area of various hydrocarbons and amino acids with the free energy of transfer of these molecules from organic solvents to water.^{16–18} In recent years, however, the attention has focused on the heat capacity of hydration of amino acids and the heat capacity of unfolding of proteins. Various studies have found a correlation between the heat capacity of hydration and the SAS.^{1,19–21} These studies have been fairly successful in predicting the heat capacity of hydration of various small molecules, including amino acids, as well as the heat capacity of protein folding, by parametrizing with respect to the accessible surface area of the solute molecules. However, these studies are less successful for binding of ligands to DNA. This discrepancy is attributable, in some cases to concomitant folding and binding,²² but for drug–DNA binding discrepancies appear to represent a breakdown of the SAS-based model for heat capacity changes. In spite of their success in predicting the heat capacity of hydration from the solvent accessible surface area, these models do not provide insight into structural or thermodynamic origin of the change in the heat capacity of hydration. In papers I and II, we have shown that a direct computation of heat capacity of hydration of even simple solutes from computer simulations is almost a prohibitively difficult task. A combination of Monte Carlo simulations and the random network model of water, however, has revealed a structural and thermodynamic view of the H-bond network properties responsible for changes in the heat capacity of hydration for various molecules. The three key properties in determining the heat capacity of hydration are the mean hydrogen bond length, the rms hydrogen bond angle, and the number of hydrogen bonds in the first hydration shell which have been perturbed. In the present work, we have found that the random network model structural parameters for the hydrogen bonds in the first hydration shell are almost the same for the four different alkanes. Consequently, the water–water interaction contribution to the heat capacity of hydration is proportional to the number of hydrogen bonds in the first shell. This provides a new parameter for the water–water

contribution to the heat capacity of hydration that is more closely related to the cause of the heat capacity changes, namely the number of hydrogen bonds perturbed in the first hydration shell. For linear alkanes, the number of hydrogen bonds perturbed in the first hydration shell (like almost every other structural or thermodynamic property) is proportional to the SAS. However, this close correspondence with SAS may not generally hold for other more heterogeneous solutes.

In the previous papers we have put forward a conjecture that the hydrogen bonds near the hydrophobic groups get perturbed so that the energy gap between the two microstates increases but not enough that it does not allow the fluctuations between these new microstates. This increase in the energy gap with still a significant fluctuation between the new energy states causes an increase in the heat capacity due to hydration of hydrophobic solutes. Thus, another insight we get from the present work is that the number of hydrogen bonds perturbed in the first hydration shell is a good measure of the microstates which have changed their energy gaps.

With the ability to relate structural and thermodynamic perturbations in the water to heat capacity changes, future directions for this work include an investigation of the relationship between SAS, number of H bonds, and heat capacity changes in polar groups or ions of different sizes and the investigation of nonadditive effects in solutes containing polar and nonpolar groups due to hydrogen bonding between waters solvating different groups.

Acknowledgment. We thank Bill Jorgensen for advice in setting up BOSS. Financial support is acknowledged from NIH (GM54105) and the E. R. Johnson Research Foundation.

References and Notes

- (1) Murphy, K.; Freire, E. *Adv. Prot. Chem.* **1992**, *43*, 313–361.
- (2) Makhatadze, G.; Privalov, P. *J. Mol. Biol.* **1990**, *213*, 385–391.
- (3) Madan, B.; Sharp, K. A. *J. Phys. Chem.* **1996**, *100*, 7713–21.
- (4) Sharp, K. A.; Madan, B. *J. Phys. Chem.* **1997**, *101*, 4343–48.
- (5) Velicelebi, G.; Sturtevant, J. M. *Biochemistry* **1979**, *18*, 1180–6.
- (6) Privalov, P. L.; Gill, S. J. *Adv. Prot. Chem.* **1988**, *39*, 191–234.
- (7) Rice, S. A.; Sceats, M. G. *J. Phys. Chem.* **1981**, *85*, 1108–1119.
- (8) Henn, A. R.; Kauzmann, W. *J. Phys. Chem.* **1989**, *93*, 3770–3783.
- (9) Sceats, M. G.; Rice, S. A. *J. Chem. Phys.* **1979**, *72*, 3248–62.
- (10) Sceats, M. G.; Stavola, M.; Rice, S. A. *J. Chem. Phys.* **1979**, *70*, 3927–38.
- (11) Sceats, M. G.; Rice, S. A. *J. Chem. Phys.* **1980**, *72*, 6183–91.
- (12) Jorgensen, W. L.; Chandrasekhar, J.; Madura, J. D.; Impey, R. W.; Klein, M. L. *J. Chem. Phys.* **1983**, *79*, 926.
- (13) Jorgensen, W. L. *Chem. Phys. Lett.* **1982**, *92*, 405.
- (14) Jorgensen, W. L. *BOSS*, Version 3.3; Yale University, New Haven, CT, 1992.
- (15) Lee, B.; Richards, F. M. *J. Mol. Biol.* **1971**, *55*, 379–400.
- (16) Hermann, R. B. *J. Phys. Chem.* **1972**, *76*, 2754–2759.
- (17) Chothia, C. *J. Mol. Biol.* **1976**, *105*, 1–14.
- (18) Tanford, C. H. *Proc. Natl. Acad. Sci.* **1979**, *76*, 4175–4176.
- (19) Livingstone, J. R.; Spolar, R. S.; Record, T. M. *Biochemistry* **1991**, *30*, 4237–4244.
- (20) Spolar, R.; Livingstone, J.; Record, M. T. *Biochemistry* **1992**, *31*, 3947–55.
- (21) Makhatadze, G.; Privalov, P. *J. Mol. Biol.* **1990**, *213*, 375–384.
- (22) Spolar, R. S.; Record, M. T. *Science* **1994**, *263*, 777–84.